

Equilibrium and dynamic moisture adsorption behaviour of bloodmeal based bioplastic

Mark Lay¹, Johan Verbeek¹ and Nicolas Koppel¹

¹School of Engineering

The University of Waikato, Private Bag 3105, Hamilton, 3240, New Zealand

Email: mclay@waikato.ac.nz, verbeek@waikato.ac.nz

Abstract— Bioplastics can be manufactured from protein or carbohydrate sources such as wheat gluten, corn, sun flower, keratin, casein, soy, gelatine and whey. A recently developed bioplastic is Novatein thermoplastic (NTP), which is produced from bloodmeal by adding water, urea, sodium sulphite, sodium dodecyl sulphate and tri-ethylene glycol (TEG), allowing it to be extruded and injection moulded. Bioplastics, compared to their petroleum counterparts, can readily adsorb or lose water, which then changes their physical properties such as tensile strength and glass transition temperature. NTP at different TEG and water contents was exposed to 20-85% relative humidity (RH) environments and change in mass recorded over 35 days to determine equilibrium and dynamic moisture adsorption behavior. Equilibrium behavior was modelled using modified Freundlich and Langmuir-Freundlich isotherms, and dynamic behavior modelled using Pilonis, Singh-Kulshrestha, exponential, Langmuir-Freundlich and simple rate equations. Excellent fits were obtained for both isotherms and the last three rate equations gave best overall fits for dynamics. NTP adsorbed up to 28% by weight in water at 85% RH, reaching equilibrium within 20 days. Plastics with high TEG had a greater affinity for water but lower water adsorption rates, while dry plastic samples had a lower adsorption rate than wet samples. The two parameter Freundlich model and the exponential or simple rate model is recommended for modelling NTP equilibrium and dynamic water adsorption.

Keywords-bioplastic; drying; bloodmeal; adsorption

I. INTRODUCTION

Renewable and compostable bioplastics have been successfully developed from different protein sources such as wheat gluten, corn, sun flower, keratin, casein, soy, gelatine and whey [1]. A recent promising bioplastic is Novatein Thermoplastic (NTP) produced from bloodmeal, a highly aggregated, cross-linked and insoluble product from the meat processing industry. This is achieved by mixing bloodmeal with urea, sodium dodecyl sulphate, sodium sulphite and tri-ethylene glycol to reduce hydrogen-bonding, hydrophobic interaction and cross-linking and increase protein chain

mobility, allowing it to melt and be extruded and injection moulded under relatively low temperatures [2, 3].

Protein based plastics tend to be hygroscopic which limits their long-term stability and affects their mechanical properties, but also improves their compostability compared to traditional plastics. For example whey based films will adsorb up to 50% by weight water at relative humidities greater than 70% [4], NTP up to 40% [5] wheat gluten up to 40% [6], polydextrose up to 40% [7], semolina up to 40% [8], and wheat flour up to 30% [6]. An additional problem is plasticisers suitable for protein plastics such as tri/poly-ethylene glycol, glycerol, and levulinic or oleic acid [9] are also hydrophilic, increasing water binding and equilibrium moisture content [9-18]. Water adsorption will reduce protein-protein interactions, resulting in the plastic transitioning to a more rubbery state with a consequent reduction in tensile strength and Young's modulus [1, 5, 9, 15, 19-26]. In addition water adsorption will increase the free volume between protein chains, increasing water diffusion into the plastic [11, 15-17, 27, 28], which consequently leads to a rapid increase in moisture content at high humidity [11].

While protein-based plastic mechanical properties can be very sensitive to changes in relative humidity, their hydroscopic nature makes them suitable for composting. Ideal moisture contents for composting is around 40 to 60%. In composting trials for NTP, unplasticised plastic samples increased in mass by water adsorption by 41% after four weeks while samples plasticised with TEG only increased by 17%, with moisture content settling to 50-60% after six weeks [29].

Knowledge of rate and extent of water adsorption is useful in determining how bio-plastics will behave in the environment in terms of predicting mechanical properties, shelf-life and compostability. Water adsorption behaviour of protein and food based materials are typically determined by exposing the material to different relative humidities over time and recording their change in mass. This provides equilibrium moisture content and the rate of adsorption or desorption. Protein based materials will typically exhibit a Type II or Type III isotherm when equilibrium moisture content is plotted against relative humidity [4, 8, 9, 30]. Type II adsorption involves the formation of a monolayer of water through chemisorption at low relative humidities, followed by multilayer adsorption at higher humidities [19] as the protein structure opens up and there is increased free volume between protein chains. Type III is typically multilayer adsorption. A

large number of equations have been developed to model adsorption equilibrium behaviour such as BET, Guggenheim, Anderson, and de Boer (GAB), Caurie, Halsey, Smith, Oswin, Bradley, Harkins–Jura, Iglesias, Henderson, Darcy Watt, Flory–Huggins, Ferro-Fontan, Park, modified GAB, and Langmuir and Freundlich [10, 12, 13, 15, 16, 18, 19, 31–34]. Verbeek and Koppel (2012) showed water adsorption in freshly injection moulded NTP and dried samples exhibited a type II/III isotherm and found the BET and Flory-Huggins isotherm fitted well with experimental data [5].

Rate of water adsorption can be found by fitting analytical type models such as the Peleg [35], Pilosof [36, 37], Singh-Kulshrestha [38] or exponential type [6] models. Alternatively, a numerical approach can be used such as by adapting the Langmuir-Freundlich model to determine rates of adsorption and desorption. The Pilosof, Singh-Kulshrestha, and exponential models have an equilibrium moisture content term thereby allowing a suitable isotherm model to be used to predict equilibrium moisture content, and the rate equations to determine how long it takes to reach equilibrium.

To achieve a good fit with a coupled kinetic/equilibrium isotherm model, an excellent fit is required for the adsorption isotherm. The Langmuir isotherm assumes monolayer, homogeneous adsorption and is well suited to modelling Type I isotherms where the sorbent has a high affinity for the sorbate. It is widely used in gas adsorption and protein adsorption in chromatography [34]. The Freundlich isotherm is suitable for non-ideal, multi-layer and heterogeneous adsorption, and is widely used for highly interactive compounds on activated carbon and molecular sieves [34]. These two models have been combined to give the Redlich-Peterson, Sips and Koble-Corrigan isotherms, also called the Langmuir-Freundlich (LF) isotherm.

The aim of this paper was to use the LF and Freundlich models to determine equilibrium adsorption behaviour of NTP at different humidities and compare the LF model to the Pilosof, Singh-Kulshrestha, and exponential models in terms of determining rate kinetics.

II. EXPERIMENTAL

A. Materials

Bloodmeal was obtained in powder form from Wallace Corporation, Hamilton, New Zealand and sieved to an average particle size of 700 μm . Technical grade sodium dodecyl sulphate (SDS) was obtained from Biolab NZ, analytical grade sodium sulphite from BDH Lab supplies and agricultural grade urea from Balance Agri-Nutrients (NZ).

B. Method

NTP was prepared by blending 100 parts by mass bloodmeal with 3 parts SDS, 3 parts sodium sulphite and 10 parts urea dissolved in water. Samples were prepared by dissolving all additives in the appropriate amount of water followed by blending with bloodmeal powder in a high speed mixer after which the required amount of plasticizer was added. The mixtures were stored over night before extrusion.

The total amount of plasticizer (water plus triethylene glycol) was kept constant at 60 parts per 100 parts bloodmeal (pphBM). Three different mass ratios of TEG to water were used, 1:1 (30 parts TEG: 30 parts water), 1:2 (25 parts TEG:35 parts water) and 5:6 (20 parts TEG:40 parts water).

Extrusion was performed using a ThermoPrism TSE-16-TC twin-screw extruder at a screw speed of 150 rpm using a temperature profile and screw configuration shown in Fig. 1. Actual melt temperatures were within 2–5 $^{\circ}\text{C}$ of the set temperatures. The extruder had a screw diameter of 16 mm, an L/D ratio of 25 and was fitted with a single 10 mm circular die. A relative torque of 50–60% of the maximum allowed in the extruder was maintained (12 Nm per screw maximum), by adjusting the mass flow rate of the feed. The extruder was fed by an oscillating trough and the extruded material was granulated using a tri-blade granulator from Castin Machinery Manufacturer Ltd., New Zealand.

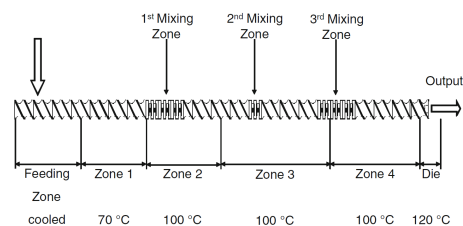


Figure 1. Extruder screw configuration and corresponding temperature profile.

Test specimens were produced using a 22 mm screw diameter BOY 15 S Injection Moulding Machine. Specimens were injected through a cold runner into a water heated mould. The shape of the tensile test specimens was in accordance with ASTM D638. A temperature profile of 70 (feed zone), 115 and 120 $^{\circ}\text{C}$ (die zone) was used employing 1200 bar injection pressure and 400 bar back pressure at screw speed of 150 min^{-1} . A 20-s cooling time was allowed in a mould locked with 30 kN locking force. Samples were injection moulded directly after extrusion and granulation, without further conditioning.

C. Sorption isotherms

Eight saturated salt solutions were prepared and placed into separate air tight containers at 18 $^{\circ}\text{C}$ to yield the required relative humidity, as outlined in Table 1.

TABLE I. SATURATED SALT SOLUTIONS USED.

Salt		Relative humidity (%)
Lithium chloride	LiCl	11.1–12.6
Potassium acetate	CH_3COOK	23.1 ± 0.3
Magnesium chloride	MgCl_2	33.1 ± 0.2
Potassium carbonate	K_2CO_3	43.2 ± 0.4
Sodium bromide	NaBr	59.1 ± 0.5
Potassium iodide	KI	69.9 ± 0.3
Sodium chloride	NaCl	75.5 ± 0.2
Potassium chloride	KCl	85.1 ± 0.3

Relative humidity was measured using a Lutron HT-3005 hygrometer. Samples for adsorption were pre-dried at 70°C for 3 days before being placed in humidity chambers. Desorption samples were placed directly into chambers after injection moulding. Moisture content was monitored gravimetrically over time; it was assumed that when three consecutive masses were observed equilibrium had been reached. Samples were left for 30–37 days to equilibrate. Final moisture content was determined gravimetrically by oven drying at 103°C for 24 h. Tests were conducted in triplicate and the averages taken.

D. Analysis

The Freundlich (1) and Langmuir-Freundlich (2) equations were used to determine water adsorption parameters K (equilibrium constant), C_{sat} (Saturation capacity, g water/g sample dry weight) and n (Freundlich parameter) (Table 2) by fitting the equations to equilibrium data (Figures 2A and B). C_{water}^* is the concentration of water in the sample (g water/g sample dry weight) at equilibrium and RH is relative humidity.

$$C_{water}^* = K \left(\frac{RH}{100} \right)^n \quad (1)$$

$$C_{water}^* = \frac{K \left(\frac{RH}{100} \right)^n C_{sat}}{1 + K \left(\frac{RH}{100} \right)^n} \quad (2)$$

Goodness of fit was calculated using the coefficient of determination (R^2) and residual sum of mean errors (RSME). Excel Solver was used to adjust parameters to maximise R^2 and minimise RSME.

To determine kinetics the non-equilibrium form of the Langmuir-Freundlich equation was used:

$$\frac{\partial C_{water}}{\partial t} = k_1 \left(\frac{RH}{100} \right)^n (C_{sat} - C_{water}) - k_2 (C_{water}) \quad (3)$$

where t is time, k_1 is the rate of adsorption and k_2 is the rate of desorption.

A simple numerical model was also used:

$$\frac{\partial C_{water}}{\partial t} = k(C_{water}^* - C_{water}) \quad (4)$$

where k is the rate of mass transfer. Both the Langmuir-Freundlich and numerical model were solved using the finite difference method with the boundary conditions at $t = 0$ for:

Dry samples: $C_{water} = 0$

Wet samples: C_{water} = measured water content of injection moulded sample

Relative humidity was assumed to remain constant over time and C_{water} was assumed to be constant throughout the plastic specimen. Therefore k in both models represents an overall mass transfer coefficient that combines diffusion of water molecules to and from the plastic surface, solid and pore

diffusion through the plastic and adsorption/desorption. A time step of 0.01 days was used.

Three analytical models were also fitted to experimental data:

The Pilosof model [36]:

$$C_{water}|_t = C_{water}|_{t=0} + \frac{(C_{water}^* - C_{water}|_{t=0})t}{B+t} \quad (5)$$

where B is the time taken for the sample to reach half the equilibrium concentration.

The Singh-Kulshrestha model [38]:

$$C_{water}|_t = C_{water}|_{t=0} + \frac{(C_{water}^* - C_{water}|_{t=0})kt}{kt+1} \quad (6)$$

where k is a mass transfer rate (1/days).

An exponential model [6]:

$$C_{water}|_t = C_{water}|_{t=0} + (C_{water}^* - C_{water}|_{t=0}) \left(1 - \exp\left(-\frac{t}{B}\right) \right) \quad (7)$$

Goodness of fit was evaluated for all five models using R^2 and RSME and k and B was adjusted using Excel solver to increase R^2 and reduce RSME.

III. RESULTS AND DISCUSSIONS

A. Adsorption isotherms

Water adsorption data for both wet and dry samples show that the 30:30 and 35:25 samples have very similar isotherms (Fig. 2 A and B), while the 40:20 samples show a lower affinity for water. Standard deviations were typically small, up to 5% of the average moisture content obtained for each condition. The exception was for the 30:30 dry samples at 20% humidity where the standard deviation was up to 50% because only a small amount of water had adsorbed onto the samples and there was a large amount of scatter. A reduced affinity for water with decreasing TEG content can be expected as TEG is well known to be hydroscopic due to its ability to form hydrogen bonds and its solubility in water. TEG is routinely used for dehydrating natural gas in the petroleum industry. The wet samples (Fig. 2 B) down to 20% humidity contain about 0.7g water per g dry weight, presumably water that is strongly bound to the protein, while for the oven dried samples, this water content is reduced to zero. The dried samples (Fig. 2 A) appear to show a Type III isotherm, where it appears that it will keep adsorbing without reaching saturation. While the wet samples show a Type II isotherm where water adsorbed initially forms a “monolayer” achieved by 20% humidity, after which it forms “multiple layers”.

To satisfactorily model “wet” samples obtained directly from the injection moulder a C_{hold} term (g water / g sample dry weight) was added to the Langmuir-Freundlich and Freundlich equations to represent water that was strongly bound to protein.

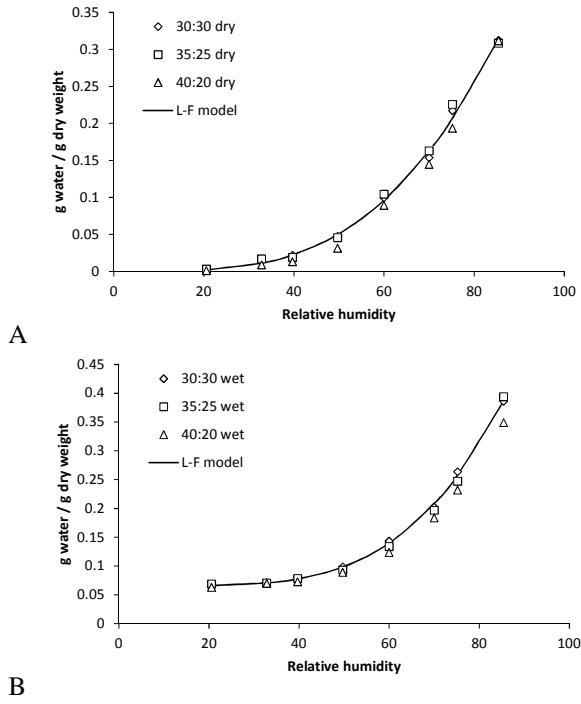


Figure 2. Equilibrium water adsorption isotherm for A. dried samples and B wet samples. Langmuir-Freundlich (L-F) model curve shown for 30:30 dry and wet data only.

$$C_{water}^* = C_{hold} + K \left(\frac{RH}{100} \right)^n \quad (8)$$

$$C_{water}^* = C_{hold} + \frac{K \left(\frac{RH}{100} \right)^n C_{sat}}{1 + K \left(\frac{RH}{100} \right)^n} \quad (9)$$

While it would be expected that bound water would decrease at humidities below 20% such as in experiments for semolina [8] and zein [9], it would be reasonable to assume atmospheric and air-conditioned room humidities would not drop below 20% (e.g. for Las Vegas) and 30-40% respectively. Three days of drying at 70°C removed bound water from the dried sample, therefore C_{hold} for the dried samples was 0.

Excellent fits between the Langmuir-Freundlich and Freundlich models and experimental data were obtained with R^2 ranging between 0.994 and 1 (Table 2 – LF best fit, Freundlich best fit), showing that the modified Langmuir-Freundlich and Freundlich equations are ideal for modelling water adsorption isotherms for NTP. In a previous paper, the GAB, BET, FH and Osw isotherms were used resulting in R^2 values of between 0.952 to 0.989 with the Osw and BET equations giving the lowest R^2 values [5]. The GAB and BET equations over predicted equilibrium water concentration in the plastic at relative humidities below 50% and under-predicted water concentrations at relative humidities above 50%. The Langmuir-Freundlich and Freundlich equations in this work showed a much better flexibility in fitting the shape of the adsorption isotherm.

TABLE II. EQUILIBRIUM PARAMETERS. Obtained by fitting equation 8 and 9 to Fig. 2A and B. $C_{hold} = 0$ for dry samples and 0.07 for wet samples.

	30:30 dry	35:25 dry	40:20 dry	30:30 wet	35:25 wet	40:20 wet
LF (Best fit)						
C_{sat}	2.82	0.8	2.95	2.63	5.68	1.29
K	0.22	1.22	0.22	0.28	0.13	0.65
n	3.58	4.19	4.06	4.43	4.71	5.12
R^2	0.997	0.997	0.998	0.999	1	1
RMSE	0.0052	0.0058	0.0041	0.0033	0.0022	0.0014
LF ($C_{sat} = 3.11$ and $K = 0.21$)						
n	3.81	3.73	4.04	4.11	4.24	4.69
C_{hold}	0	0	0	0.07	0.07	0.07
R^2	0.995	0.992	0.998	0.997	0.993	1
RMSE	0.007	0.0094	0.0041	0.0054	0.0092	0.0018
LF ($C_{sat} = 1.28$ and $n = 4.48$)						
K	0.69	0.7	0.65	0.65	0.64	0.55
R^2	0.991	0.986	0.998	0.997	0.989	0.994
RMSE	0.0099	0.0126	0.0044	0.0057	0.0112	0.007
LF ($K = 0.31$ and $n = 4.18$)						
C_{sat}	2.34	2.37	2.24	2.26	2.23	1.95
R^2	0.99	0.983	0.998	0.997	0.99	0.993
RMSE	0.0102	0.0135	0.0041	0.0054	0.0108	0.0081
Freundlich (Best fit)						
K	0.54	0.53	0.57	0.62	0.67	0.57
n	3.35	3.22	3.82	4.12	4.55	4.44
R^2	0.997	0.994	0.998	0.999	1	0.999
RMSE	0.0055	0.0078	0.0044	0.0037	0.0018	0.0024
Freundlich ($K = 0.57$)						
n	3.58	3.51	3.84	3.86	3.98	4.44
R^2	0.995	0.991	0.998	0.997	0.993	0.999
RMSE	0.0072	0.01	0.0044	0.0058	0.0093	0.0024
Freundlich ($n = 3.85$)						
K	0.6	0.61	0.57	0.58	0.57	0.5
R^2	0.99	0.982	0.998	0.997	0.991	0.992
RMSE	0.0103	0.014	0.0044	0.0056	0.0104	0.0082

C_{sat} ranged between 0.8 and 5.68 g water per g dry weight (Table 2 – LF Best fit). This implies that given the opportunity, NTP will be saturated with water between 45-85% moisture content, i.e. when it is a slurry in the extreme cases. Fortunately, this will not occur unless the plastic is placed in a water bath, which makes the C_{sat} term physically meaningless. Therefore the Freundlich equation is better suited because it has less terms, but it is empirical compared to the Langmuir equation which at least has a theoretical basis.

K represents the affinity of the solid towards the sorbent, i.e. the higher the K the greater the affinity, while n represents the favourability of the adsorption. A low n below 1 implies chemisorption, typical for Type I isotherms, while an n above 1 implies cooperative adsorption, typical for Type II, III [34] or Type V. In both cases, the high n value and isotherm curve shape suggest cooperative adsorption where initially protein has to be opened up by water to increase regions available for adsorption. Unfortunately, while the Langmuir-Freundlich and Freundlich models gave excellent fits, they also allowed for a range of K , C_{sat} and n that can be fitted to the data with equally good R^2 , which prevents a direct comparison between sample types and conditions and their effect on the isotherm parameters. Therefore to determine the effect of pre-drying and plasticiser content on the equilibrium parameters, isotherm curves were fitted by varying one parameter out of K , C_{sat} and n across all plasticiser contents and wet and dry samples and making the remainder constant (Table 2).

For both dried and wet samples, the equilibrium isotherm became less favourable with decreasing TEG, shown by a decreasing C_{sat} and K and increasing n (with the exception for 35:25 dry where n decreased). A decreasing K indicates a reduced affinity for water and is shown by a decrease in the slope of the isotherm. As was stated before, TEG has a strong affinity for water, therefore decreasing TEG will reduce the plastic's affinity for water. Increasing C_{sat} with increasing TEG can be explained by the TEG providing additional sites for hydrogen bonding by the water and also increasing the free volume of the plastic, also increasing adsorption sites. Parameters for 30:30 and 35:25 dry and for 30:30 and 35:25 wet were similar indicating that TEG's effect on NTP's affinity for water decreased or plateaued with increasing TEG concentration.

B. Adsorption kinetics

As the Langmuir-Freundlich model allowed for a range of K , C_{sat} and n that can be fitted to the data with equally good R^2 , this then impacts on the rate constant, k_1 , used to fit the kinetic data, as adsorption curves which look similar will have quite different k_1 depending on the equilibrium parameters that were fitted to the isotherm. This prevents direct comparison of rate constants for the different plasticiser contents and wet and dry samples. Therefore Pilosof, Singh-Kulshrestha, exponential and numerical models were used to fit the kinetic data using the plastic equilibrium water concentration predicted by the Langmuir-Freundlich model. Parameters obtained and goodness of fit are shown in Table 3. Example experimental data and model curves for concentration of water in the plastic with time are shown in Fig. 3 and 4.

TABLE III. KINETIC PARAMETERS. Average k and B values for each plasticiser content for wet and dry samples are averaged from values for 60, 70, 75.2 and 85.4 humidities. R^2 and RSME for each model and condition were evaluated by comparing model and experimental data for all humidities.

	30:30 dry	35:25 dry	40:20 dry	30:30 wet	35:25 wet	40:20 wet
Pilsof model						
B	3.578	3.365	2.71	2.777	3.4	2.742
R^2	0.982	0.986	0.989	0.993	0.994	0.989
RMSE	0.011	0.01	0.009	0.007	0.007	0.008
Singh-Kulshrestha model						
k	0.287	0.3	0.372	0.425	1.226	2.175
R^2	0.981	0.985	0.986	0.993	0.994	0.989
RMSE	0.012	0.01	0.01	0.007	0.007	0.008
Exponential model						
B	7.404	7.072	6.102	6.065	6.434	4.927
R^2	0.998	0.998	0.998	0.993	0.993	0.985
RMSE	0.004	0.004	0.004	0.007	0.007	0.009
Numerical model						
k	0.136	0.142	0.164	0.174	0.208	0.454
R^2	0.998	0.998	0.998	0.993	0.993	0.982
RMSE	0.004	0.004	0.004	0.007	0.007	0.01

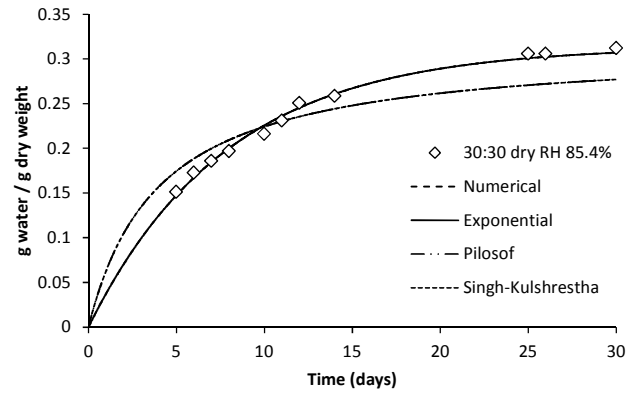


Figure 3. Comparison of the numerical, exponential, Pilosof and Singh-Kulshrestha models to experimental data for 30:30 dry samples at a relative humidity of 85.4%. The numerical and exponential models overlap each other over the experimental data and the Pilosof and Singh-Kulshrestha models overlap.

The Pilosof and Singh-Kulshrestha models over-estimated the initial adsorption rates for dry samples (Fig. 3), resulting in R^2 values of 0.982 to 0.989 for the dry samples (Table 3). The goodness of fit for wet samples was generally better than for the dry samples, indicating both models could be used satisfactorily for the wet samples.

The exponential and numerical model and experimental data showed excellent fits for dried samples indicated by the high R^2 values (0.998) and low RSME (0.004). The goodness of fit for the wet samples was slightly less with R^2 values between 0.982 and 0.993 and RSME between 0.0070 and 0.0101. The worst fits were for 40:20 wet curves, where it appears that water adsorption was not occurring between 0 and 5 days for the samples at 85% humidity and water concentration dipped initially for the samples at 75% humidity and then increased (Fig. 4). It is uncertain why this might have occurred, but given that each data point is an average of three samples, it points to there being an issue with the specimens or experimental setup for these conditions.

For the dry samples, $1/B$ from the Pilosof matches closely with the k value from the Singh-Kulshrestha model and likewise for the exponential and numerical model. For the wet samples, the match was not as good generally being higher or lower by as much as 0.2 for the Singh-Kulshrestha and Pilosof models. For the exponential and numerical model, the match within 0.05 for the 30:30 wet and 35:25 wet samples, but was out by 0.25 for the 40:20 wet sample. The disparity is likely due to the greater difficulty in fitting the models to the wet sample data which was of poorer quality compared to the dry sample data. Where the data is good and a good fit is achieved, rate parameters can be obtained from the exponential model and used reliably in the numerical model.

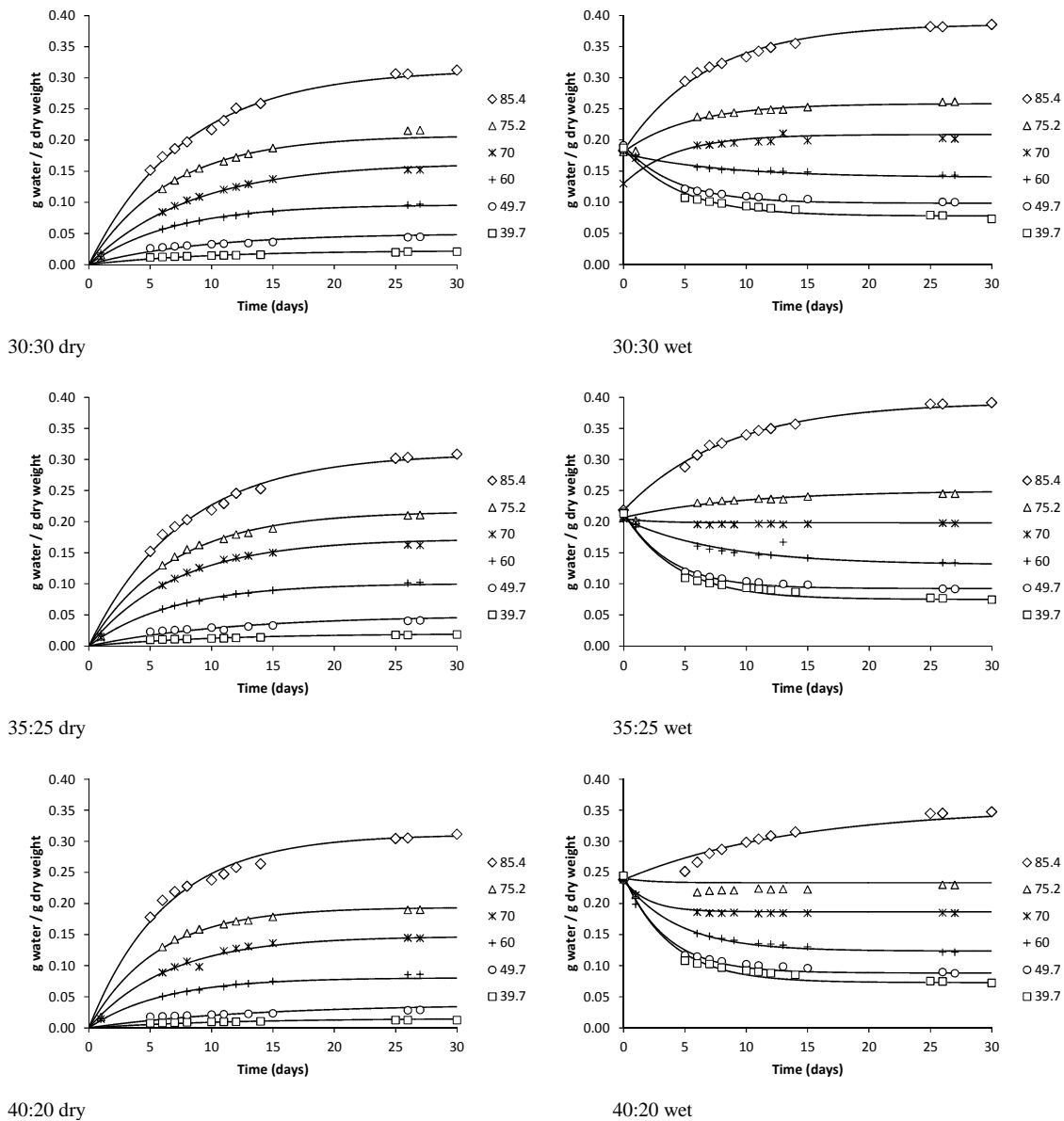


Figure 4. Comparison of the numerical model and experimental data for change in water concentration in pre-dried and wet plastic samples at different plasticiser contents (water:TEG) and humidities. For clarity, the curves for 20.6 and 32.8% relative humidities have been omitted.

At 85% humidity water concentration increased up to 0.39 g water per g dry weight, reaching 90% of the final water concentration within 15 days. Water adsorption will result in the protein plastic transitioning from a glassy structure to a rubbery structure with lower mechanical properties [5, 9]. Equilibrium in all cases was reached within 25-30 days.

Adsorption rate decreased with increasing TEG for pre-dried and wet samples (shown by the decrease in k and increase in B , Table 6). This could be due to TEG restricting water diffusion into the sample due to stronger H-bonding interaction between it and the water than between the water and protein. Water and ethylene glycol have been shown to form H-bonded structures where the hydroxyl oxygen atoms will complex with two water molecules, forming a hexatomic ring that strengthens water-ethylene glycol H-bonding [28].

Wet samples showed a higher adsorption rate (shown by a higher k and decrease in B , Table 6), likely due to a more open protein structure due to greater hydration of the protein, compared to pre-dried specimens where the water of hydration between/within proteins has been reduced. Drying would result in greater H-bonding between/within the proteins, resulting in a more closed structure restricting water diffusion. Drying by heating can cause unfolding of proteins resulting in a more hydrophobic structure, also reducing water uptake [39]. Subsequent work to this paper looking at the effect of heating on NTP protein structure using the infra-red beamline at the Australian Synchrotron showed heating over time increased β -sheet structures in the proteins. β -sheet structures are stabilised by H-bonding, hence sites for H-bonding by water would be no longer available resulting in less water diffusion and lower water sorption capacity.

C. Implications

In humid environments, conditioned NTP will adsorb up to 26-30% by weight water, reaching 90% of its final weight within 15 days (this will depend on the shape and thickness of the product), resulting in a more rubbery structure with lower mechanical strength. Conversely, water desorption in dry environments such as air conditioned rooms will result in the plastic becoming more brittle. For NTP to be stable and prevent a change in mechanical properties in humid or dry environments, it will either need to be coated with a protective layer to reduce or prevent moisture uptake, or the water replaced with a less volatile plasticiser or TEG replaced with a more water resistant plasticiser. Generally coatings would not be ideal because water adsorption/desorption could occur in localised areas where the coating has been scratched. As an example for a plasticiser, Lawton (2004) showed using dibutyl tartrate as a plasticiser for zein films had a much lower loss in tensile strength and Young's modulus at humidities between than 20-60% than when TEG was used [9].

Conversely, for rapid composting/biodegradation, rapid water uptake and high equilibrium moisture content is good. In the conditions explored, NTP never reached the 40% moisture content when exposed to air but it reached 28% moisture content for the wet samples (0.39 g/g dry weight for 35:25 wet samples within 25-30 days at 85% humidity. Therefore, if disposed of on the ground, landfill or compost in a wet environment, NTP should begin to degrade readily after three to four weeks (see [29]).

CONCLUSIONS

This work showed that the modified Langmuir-Freundlich and Freundlich isotherm was excellent for modelling water adsorption equilibrium behavior for NTP. A relatively simple rate kinetic model or exponential model coupled with the Langmuir-Freundlich isotherm is suitable for predicting moisture adsorption/desorption with time. These two models could then be coupled with another model that predicts plastic mechanical properties based on water content. This would then allow predictions of how NTP would behave in specific applications in environments with changing humidities. This would then allow some assessment of the suitability of NTP for specific applications. The Pilosof and Singh-Kulshrestha kinetic models over-predicted the rate of adsorption resulting in a worse fit than the simple rate model or the exponential model. However, all models performed similarly for modelling desorption.

References

- [1] Verbeek, C.J.R. and L.E. van den Berg, Extrusion Processing and Properties of Protein-Based Thermoplastics. *Macromolecular Materials and Engineering*, 2009. 295(1): p. 10-21.
- [2] Verbeek, C.J.R., et al., *Plastics material*. 2009, WaikatoLink Ltd, New Zealand: New Zealand.
- [3] Verbeek, C. and L. van den Berg, Development of Proteinous Bioplastics Using Bloodmeal. *Journal of Polymers and the Environment*, 2010: p. 1-10.
- [4] Kim, S.J. and Z. Ustunol, Solubility and Moisture Sorption Isotherms of Whey-Protein-Based Edible Films as Influenced by Lipid and Plasticizer Incorporation. *Journal of Agricultural and Food Chemistry*, 2001. 49(9): p. 4388-4391.
- [5] Verbeek, C.R. and N. Koppel, Moisture sorption and plasticization of bloodmeal-based thermoplastics. *Journal of Materials Science*, 2012. 47(3): p. 1187-1195.
- [6] Roman-Gutierrez, A.D., S. Guilbert, and B. Cuq, Distribution of Water between Wheat Flour Components: A Dynamic Water Vapour Adsorption Study. *Journal of Cereal Science*, 2002. 36(3): p. 347-355.
- [7] Li, Q.E. and S.J. Schmidt, Use of Ramping and Equilibrium Water Vapor Sorption Methods to Determine the Critical Relative Humidity at which the Glassy to Rubbery Transition Occurs in Polydextrose. *Journal of Food Science*, 2011. 76(1): p. E149-E157.
- [8] Hébrard, A., et al., Hydration properties of durum wheat semolina: influence of particle size and temperature. *Powder Technology*, 2003. 130(1-3): p. 211-218.
- [9] Lawton, J.W., Plasticizers for Zein: Their Effect on Tensile Properties and Water Absorption of Zein Films. *Cereal Chemistry Journal*, 2004. 81(1): p. 1-5.
- [10] Maria Martelli, S., et al., Influence of plasticizers on the water sorption isotherms and water vapor permeability of chicken feather keratin films. *LWT - Food Science and Technology*, 2006. 39(3): p. 292-301.
- [11] Perdomo, J., et al., Glass transition temperatures and water sorption isotherms of cassava starch. *Carbohydrate Polymers*, 2009. 76(2): p. 305-313.
- [12] Cassini, A.S., L.D.F. Marczak, and C.P.Z. Norena, Water adsorption isotherms of texturized soy protein. *Journal of Food Engineering*, 2006. 77(1): p. 194-199.
- [13] Brett, B., et al., Moisture Sorption Characteristics of Starchy Products: Oat Flour and Rice Flour. *Food Biophysics*, 2009. 4(3): p. 151-157.
- [14] Su, J.-F., et al., Moisture sorption and water vapor permeability of soy protein isolate/poly(vinyl alcohol)/glycerol blend films. *Industrial Crops and Products*, 2009. 31(2): p. 266-276.
- [15] Kristo, E. and C.G. Biliaderis, Water sorption and thermo-mechanical properties of water/sorbitol-plasticized composite biopolymer films: Caseinate-pullulan bilayers and blends. *Food Hydrocolloids*, 2006. 20(7): p. 1057-1071.
- [16] Mali, S., et al., Water sorption and mechanical properties of cassava starch films and their relation to plasticizing effect. *Carbohydrate Polymers*, 2005. 60(3): p. 283-289.
- [17] Fabra, M.J., P. Talens, and A. Chiralt, Water sorption isotherms and phase transitions of sodium caseinate-lipid films as affected by lipid interactions. *Food Hydrocolloids*. 24(4): p. 384-391.
- [18] Jangchud, A. and M.S. Chinnan, Properties of Peanut Protein Film: Sorption Isotherm and Plasticizer Effect. *Lebensmittel-Wissenschaft und-Technologie*, 1999. 32(2): p. 89-94.
- [19] Zhang, Y. and J. Han, Sorption Isotherm and Plasticization Effect of Moisture and Plasticizers in Pea Starch Film. *Journal of Food Science*, 2008. 73(7): p. E313-E324.
- [20] Verbeek, C.J. and L.E. Van Den Berg, Recent Developments in Thermo-Mechanical Processing of Proteinous Bioplastics. *Recent Patents on Materials Science*, 2009. 2(3).
- [21] Sharma, S., J.N. Hodges, and I. Luzinov, Biodegradable plastics from animal protein coproducts: Feathermeal. *Journal of Applied Polymer Science*, 2008. 110(1): p. 459-467.
- [22] Swain, S.N., K.K. Rao, and P.L. Nayak, Biodegradable polymers. III. Spectral, thermal, mechanical, and morphological properties of cross-linked furfural-soy protein concentrate. *Journal of Applied Polymer Science*, 2004. 93(6): p. 2590-2596.
- [23] Zhang, J., P. Mungara, and J. Jane, Mechanical and thermal properties of extruded soy protein sheets. *Polymer*, 2001. 42(6): p. 2569-2578.
- [24] Pomet, M., et al., Intrinsic influence of various plasticizers on functional properties and reactivity of wheat gluten thermoplastic materials. *Journal of Cereal Science*, 2005. 42(1): p. 81-91.
- [25] Ortiz, M.E.R., E. San Martin-Martinez, and L.P.M. Padilla, Rheological and Thermal Properties of Extruded Mixtures of Rice Starch and Isolated Soy Protein. *Starch-Starke*, 2008. 60(10): p. 577-587.
- [26] Hochstetter, A., et al., Properties of gluten-based sheet produced by twin-screw extruder. *LWT - Food Science and Technology*, 2006. 39(8): p. 893-901.

- [27] Cho, S.Y. and C. Rhee, Sorption Characteristics of Soy Protein Films and their Relation to Mechanical Properties. *Lebensmittel-Wissenschaft und-Technologie*, 2002. 35(2): p. 151-157.
- [28] Zhang, J., et al., Hydrogen bonding interactions between ethylene glycol and water: density, excess molar volume, and spectral study. *Science in China Series B: Chemistry*, 2008. 51(5): p. 420-426.
- [29] Verbeek, C.R., T. Hicks, and A. Langdon, Biodegradation of Bloodmeal-Based Thermoplastics in Green-Waste Composting. *Journal of Polymers and the Environment*, 2012. 20(1): p. 53-62.
- [30] Ganesan, V., K.A. Rosentrater, and K. Muthukumarappan, Dynamic Water Adsorption Characteristics of Distillers Dried Grains with Solubles (DDGS). *Cereal Chemistry Journal*, 2007. 84(6): p. 548-555.
- [31] Srinivasa, P.C., et al., Properties and sorption studies of chitosan-polyvinyl alcohol blend films. *Carbohydrate Polymers*, 2003. 53(4): p. 431-438.
- [32] Alix, S., et al., Effect of chemical treatments on water sorption and mechanical properties of flax fibres. *Bioresource Technology*, 2009. 100(20): p. 4742-4749.
- [33] Sopade, P.A., et al., Moisture-sorption isotherms of irish and sweet potatoes. *Journal of Food Process Engineering*. 33(Compendex): p. 385-397.
- [34] Foo, K.Y. and B.H. Hameed, Insights into the modeling of adsorption isotherm systems. *Chemical Engineering Journal*, 2010. 156(1): p. 2-10.
- [35] Peleg, M., An empirical model for description of moisture sorption curves. *Journal of Food Science*, 1988. 53: p. 1216-1219.
- [36] Pilosof, A.M.R., R. Boquet, and G.B. Bartholomai, Kinetics of Water Uptake by Food Powders. *Journal of Food Science*, 1985. 50(1): p. 278-279.
- [37] Elizalde, B.E., A.M.R. Pilosof, and G.B. Bartholomai, Empirical Model for Water Uptake and Hydration Rate of Food Powders by Sorption and Baumann Methods. *Journal of Food Science*, 1996. 61(2): p. 407-409.
- [38] Singh, B.P.N. and S.P. Kulshrestha, Kinetics of water sorption by soybean and pigeonpea grains. *Journal of Food Science*, 1987. 52: p. 1538-1541.
- [39] Kalapathy, U., N.S. Hettiarachchy, and K.C. Rhee, Effect of drying methods on molecular properties and functionalities of disulfide bond-cleaved soy proteins. *Journal of the American Oil Chemists' Society*, 1997. 74(3): p. 195-199.